Concentration Fluctuations and Surface Adsorption in Hydrogen-Bonded Mixtures

Ana Díez-Pascual, Francisco Ortega, Amalia Crespo-Colín, Aurora Compostizo, Francisco Monroy, and Ramón G. Rubio*

Departamento Química Física I, Facultad de Química, Universidad Complutense, 28040-Madrid, Spain

Received: March 30, 2004; In Final Form: April 22, 2004

Concentration fluctuations of the 1,4-butanediol + 1-dodecanol mixture have been characterized by laser light-scattering experiments at two temperatures. The results show that both components have a clear tendency toward heterocoordination that increases with temperature. The combination of the concentration fluctuation results with the surface tension measurements have provided precise values of the excess surface adsorption Γ_{21} as a function of the composition. Γ_{21} shows a maximum for a mole fraction of 1-dodecanol of $x_2 \approx 0.02$; the maximum of Γ_{21} decreases with increasing temperature. The position of this maximum contrasts with that at which the local compositions show extrema in the bulk. The surface entropy versus the composition curve shows maxima and minima throughout the composition range. This behavior resembles that found for some water−alcohol mixtures. Using the experimental surface tension data, we predicted the excess surface adsorption using a lattice-fluid model that takes into account the existence of hydrogen bonds between the two components. In spite of the fact that the model accounts reasonably well for the volumetric properties of the system, poor predictions are obtained for Γ_{21}.

Introduction

The surface tension's dependence on the composition, γ, of liquid mixtures is often required for rational chemical process design, and it is of great relevance to biological processes.[1] When the components of a mixture have rather different values of γ, there usually is a tendency for preferential adsorption of the component with the lowest surface tension at the air−liquid interface. This preferential adsorption is tuned by the nonideality (excess Gibbs energy) of the mixture. The composition and structure of the adsorbed surface films may differ significantly, depending on the type of molecular interactions that exist between the molecules of the mixture, the density of packing, and the molecular shape.[2−4] These three factors are also responsible for the difference between the overall composition and the local composition in the immediate vicinity of a molecule in a binary mixture. However, for a given mixture one of the factors may be more important for the surface than for the bulk segregation, for example, hydrogen bonding can be achieved more efficiently in the bulk than at the interface.

For a fluid mixture at constant temperature and pressure, the relationship between γ and the surface excess of component 2 with respect to component 1, Γ_{21}, is given by the Gibbs equation[1]

$$\Gamma_{21} = -\frac{\left(\frac{\partial\gamma}{\partial x_2}\right)_{T,P}}{\left(\frac{\partial\mu_2}{\partial x_2}\right)_{T,P}} \tag{1}$$

where $\chi_T = (\partial\mu_2/\partial x_2)_{T,P}$ is the osmotic compressibility and μ_2 is the chemical potential of component 2 at mole fraction x_2. Therefore, Γ_{21} can be calculated if the composition's dependence on γ and of μ_2 is known. The connection between bulk and surface segregation is clearly pointed out by considering that concentration fluctuations and nonrandomness in binary mixtures can be described in terms of the concentration−concentration correlation function S_{cc} (i.e., the structure factor at zero wavevector),[5,6] which is directly related to the osmotic compressibility:[7]

$$S_{cc}^{-1} = \frac{1}{x_1 x_2}\left[\frac{\partial\left(\frac{\mu_2}{RT}\right)}{\partial \ln x_2}\right]_{T,P} \tag{2}$$

S_{cc} is also closely related to the so-called Kirkwood−Buff integrals that fully describe the equilibrium properties of fluid mixtures.[8−10]

Strey et al.[11] have shown that assuming ideal behavior to calculate the osmotic compressibility may be inadequate when calculating surface adsorption, even for dilute water−alcohol mixtures, thus an estimation of μ_2 is necessary. In refs 2, 3, and 11, the activity of the solute a_2 [$\mu_2(x_2, T) = \mu_2^0(T) + RT \ln a_2(x_2,T)$, with μ_2^0 being the chemical potential at the reference state] has been estimated from the vapor pressure data.[12] To do so, it is necessary to carry out a second derivative of the Gibbs energy with respect to x_2, which may introduce a noticeable uncertainty into $(\partial\mu_2/\partial x_2)$ unless the vapor pressure data are highly precise.[3] Moreover, in a recent paper using small-angle neutron scattering, Almasy et al.[13] have shown that small inaccuracies in the G^E results may lead to large errors in the osmotic compressibility. More recently,[14,15] the activity coefficients, needed to calculate μ_2 at each x_2, have been evaluated using approximate liquid-solution models such as UNIFAC, NRTL, and so forth.[12] In spite of the fact that such models are convenient because the parameters needed for calculating μ_2 are available for many mixtures, their ability to predict the Gibbs energy of the mixtures is, in many cases, poor.[16] As a consequence, the values of $(\partial\mu_2/\partial x_2)$ obtained may be in great error, thus leading to unsatisfactory Γ_{21} predictions. More recently, the opposite strategy has been explored, and the activity coefficients at infinite dilution have been calculated from surface tension data in combination with eq 1.[17]

* Corresponding author. E-mail: rgrubio@quim.ucm.es.

10.1021/jp048622k CCC: $27.50
Published on Web 06/05/2004

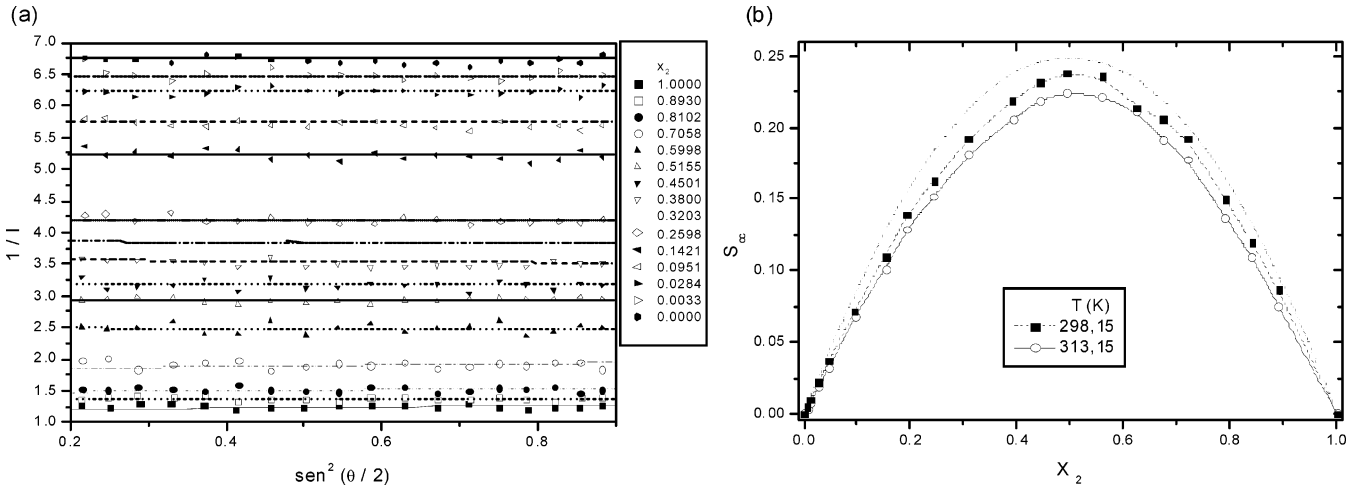

Figure 1. (a) Ornstein−Zernike plot of the intensity of the scattered light I vs the scattering angle θ. The symbols correspond to different concentrations. As can be observed, I is not dependent on θ. The lines are the best fits of the data to horizontal straight lines. (b) Concentration−concentration correlation function S_{cc} for the BDO−DO mixture as a function of x_2. The symbols represent the experimental measurements, and the dotted line represents the ideal mixture's behavior: $S_{cc} = x_1x_2$.

It is well known that the light-scattering technique is well suited for obtaining the osmotic compressibility of binary mixtures.[18] Therefore, the combination of light-scattering and surface-tension data for binary mixtures is adequate for obtaining reasonably precise surface adsorption data in mixtures. These can be used to test the reliability of some of the above-mentioned liquid-mixture models for calculating Γ_{21} from surface tension data. Moreover, the local composition problem has recently been discussed in terms of approximate mixture models for some binary mixtures.[9,10] Light-scattering experiments may also shed light on this problem.

The purpose of this paper is to report precise surface adsorption data for the mixture 1,4-butanediol (1) + 1-dodecanol (2) (BDO−DO) over the whole range of concentration. This system has been chosen for three reasons: (a) it is known that, in general, alcohol systems present complex behavior in their local compositions,[10,19] (b) because the BDO−DO system presents an important change in the dielectric permittivity with concentration,[20] which may control the interactions between the two kinds of molecules, and (c) because both components show a large difference in surface tension. Because hydrogen bonding is temperature sensitive, the proposed study has been carried out between 295 and 330 K. The results have been compared with the predictions of a lattice-fluid theory for hydrogen-bonded fluids proposed by Panayiotou and Sanchez.[21]

The results will show that there is a preferential adsorption of 1-dodecanol at the air−liquid interface. Γ_{12} increases with x_2 for highly dilute mixtures and shows a maximum at $x_2 \approx 0.02$. For a given concentration, Γ_{21} slightly decreases as the temperature is increased. In the bulk, the two components have a clear tendency to heterocoordinate, but the value of x_2, at which there is a maximum tendency of DO to be surrounded by BDO molecules, is much higher than the maximum in Γ_{21}. In spite that the theory is able to describe reasonably well the volumetric properties of the system resonably well; it does not correctly predict the osmotic susceptibility, thus leading to unsatisfactory results for the surface adsorption and for the bulk local compositions.

Experimental Section

The light-scattering experiments were performed at 298.15 K using a Malvern 4700 instrument and a Coherent 300 Ar^+ laser working at 514.5 nm. The precision of the intensity of the scattered light measured at a given angle is better than 3%; however, the average of the measured angles rises to slightly <5%. The osmotic compressibility was calculated as indicated in the Appendix, its precision being better than 5%. The refractive index was measured with a Carl Zeiss refractometer at six wavelengths between 404.7 and 656.3 nm (precision of n at 514.5 nm was $\pm 3 \times 10^{-5}$). The values at 623.8 nm were calculated from the Cauchy equation.[22] The densities were measured using an Anton-Paar DMA 620 vibrating-tube densimeter (precision of ρ was $\pm 2 \times 10^{-5}$ g·cm^{-3}). The surface tension experiments were carried out using a Krüus K-10 ST tensiometer using the plate method. The measurement cell was modified to minimize the evaporation of the sample.[23] Each experimental data point is the average of five readings taken in 10-min intervals. The reproducibility of the results was better than ± 0.03 mN·m^{-1}. The mixtures were prepared by weight in an analytical balance with a precision of ± 0.01 mg. The uncertainty in the mole fraction was estimated to be ± 0.0001. The temperature in both techniques was kept constant by circulating water from an external bath and was controlled to within ± 0.005 K.

1,4-Butanediol and 1-dodecane were purchased from Aldrich and have nominal purities higher than 99 mol %. The densities and surface tensions of the pure components at 298.15 K agreed well with values published in the literature.[24]

TABLE 1: Coefficients that Give the Best-Fit S_{cc} Data to the Redlich−Kister Equation[a]

T (K)	A_0	$-A_1$	$-A_2$	A_3
298.15	0.941 ± 0.004	0.033 ± 0.009	0.13 ± 0.02	
330.15	0.895 ± 0.003	0.05 ± 0.01	0.20 ± 0.01	0.09 ± 0.03

[a] Equation 3.

Results

Static Light Scattering. Figure 1a shows the Ornstein−Zernike plot of the intensity of the scattered light for the BDO−DO mixture at 298.15 K as a function of the mole fraction of DO. It can be observed that, within the experimental uncertainty, there is no angle dependence of I. Similar results were obtained at 313.15 K.

The S_{cc} curves were calculated as described in the Appendix, and the results are shown in Figure 1b. In ideal mixtures with a random distribution of molecules, S_{cc} takes a very simple

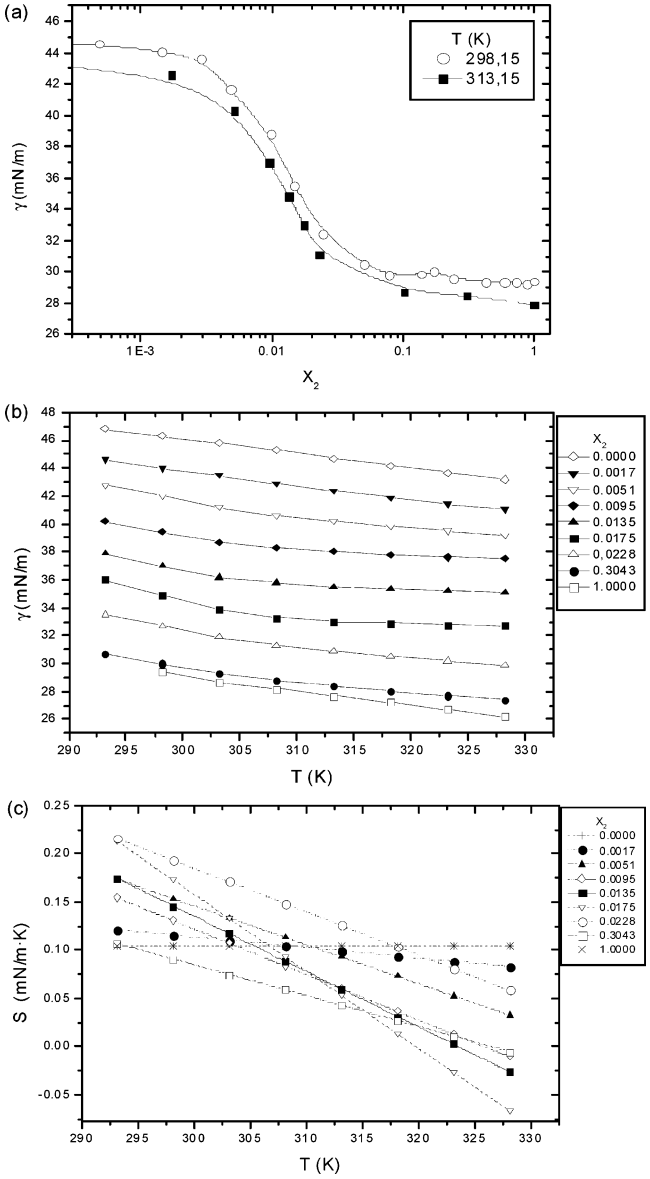

Figure 2. (a) Concentration dependence of the surface tension γ. (b) Temperature dependence of γ for different concentrations. (c) Temperature dependence of the surface entropy for different concentrations. Notice that the values for both pure components are coincident. The lines are aids for the eye.

form: $S_{cc} = x_2(1 - x_2)$; that is, S_{cc} is a symmetric parabola when plotted against x_2 with a maximum at $S_{cc} = 0.25$ and $x_2 = 0.5$. For the present system, $S_{cc} < 0.25$, which indicates that the molecules have a clear tendency to heterocoordinate;[6] that is, the local value of x_1 in the immediate vicinity of one molecule of type 1 is lower than the overall value of x_1 in the mixture. This behavior is qualitatively different from that reported for the system methanol−1-decanol.[25] The increase in T leads to a small decrease in S_{cc}. This is somewhat unexpected and probably indicates that the increase in the thermal energy has a stronger effect in breaking the hydrogen bonds between the BDO molecules than between DO and BDO−DO. We have fit the experimental data to the Redlich−Kister equation:

$$S_{cc} = x_2(1 - x_2)\sum_i A_i(1 - 2x_2)^{i-1} \qquad (3)$$

Table 1 contains the values of the A_i constants that give the best-fit data at the two temperatures. The low scattering of the

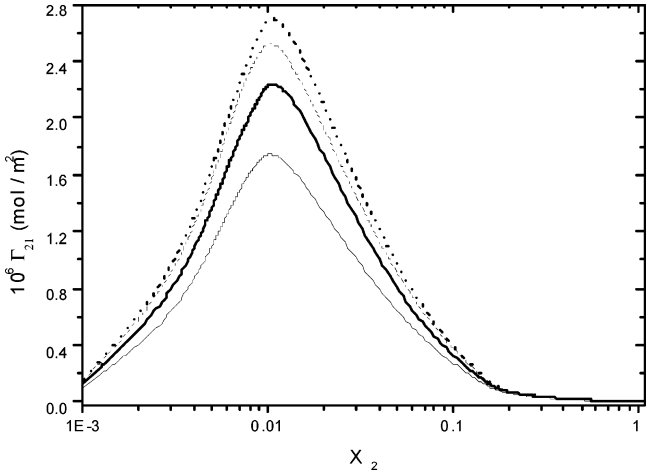

Figure 3. Concentration dependence of the relative surface adsorption Γ_{21}. The continuous lines represent the results for the BDO−DO mixture, and the dotted lines represent the values calculated by assuming ideal mixture behavior. The thick lines correspond to 298.15 K, and the thin lines correspond to 313.15 K.

S_{cc} values shown in Figure 1b is a good indication that the light-scattering technique provides accurate values of $(\partial\mu_2/\partial x_2)$.

Surface Tension. Figure 2a shows the surface tension γ as a function of composition, and at 298.15 K, it can be observed that small amounts of DO strongly reduce the surface tension of the mixture. The excess surface tension results have been fit to a Pade approximate-type equation with an average standard deviation of ± 0.6 mN·m^{-1}. Figure 2b shows γ for mixtures diluted in DO as a function of temperature; even though the pure components show linear behavior, we observed that dilute mixtures as a function of temperature show nonlinear behavior. These results allow one to calculate the surface entropy, $S^\gamma = -((\mathrm{d}\gamma/\mathrm{d}T))_{x_2}$. The results are shown in Figure 2c and point out that there is a strong difference between the surface behavior of the pure components (which have identical values of S^γ) and that of the mixtures. Similar conclusions were obtained for the surface enthalpy.

Discussion

Relative Surface Adsorption. The relative adsorption of component 2, Γ_{21}, has been calculated from the S_{cc} and the γ versus x_2 curves according to eq 1, and the results are shown in Figure 3. They show that Γ_{21} rises with x_2 for very dilute mixtures and that Γ_{21} shows a maximum in the low DO concentration range ($x_2 \approx 0.02$). This qualitative behavior is expected for mixtures of two components with different surface tensions.[26] The Figure also includes the Γ_{21} calculated without taking into account the effect of the nonideal behavior of the mixture. The ideal behavior overestimates the maximum of Γ_{21} by 20% at 298 K and by 30% at 313 K. As can be observed, the effect of T on Γ_{21} is larger than for the case when ideal is assumed. It must be remarked that the effect of the change of $(\partial\gamma/\partial x_2)$ with T on the change of Γ_{21} is 4% at the maximum (ca. 1% for most of the concentration range), whereas the effect of the RT term is <10%. Thus, a significant part of the change of Γ_{21} arises from the change of $(\partial\mu_2/\partial x_2)$.

Figure 4 shows the complex concentration dependence of S^γ, which is qualitatively similar to that described for the water−1,2-pentanediol mixture but different from that of the water−*n*-butanol mixture.[27] Also, the nitromethane−*n*-heptane mixture shows S^γ behavior similar to that shown in Figure 4; however, the authors did not obtain data for x_2 higher than 0.02, thus they observed only the first minimum of the curve.[28] In refs 27

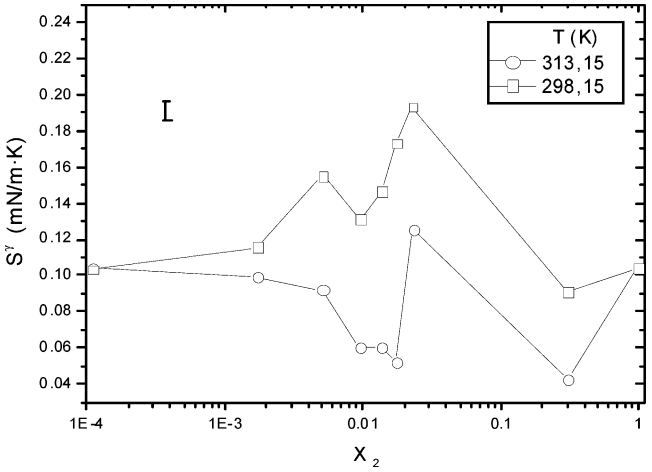

Figure 4. Surface entropy of the mixture as a function of concentration. Notice that the maximum at $x_2 \approx 0.02$ corresponds to the maximum of Γ_{21}. The bar indicates the estimated uncertainty in S^γ.

and 28, it is speculated that the observed behavior of S^γ in the dilute regime might be due to the existence of packing transitions of the solvent (1,2-pentanediol and *n*-heptane) at the surface as the bulk concentration is increased. The maximum of Γ_{21} is found at concentrations very close to the second maximum of S^γ. More recently, Jerie et al.[29] have reported the formation of clathrate-like structures for a 1-hexanol−ethylene glycol mixture.

Bulk Local Compositions. The excess (or deficit) number of molecules *j* in the immediate vicinity of a molecule of species *i*, Δn_{ij}, is defined with respect to a reference state in which the volume occupied by the excess *i* molecules around an *i* molecule is equal to the volume left free by the *j* molecules around the same *i* molecule.[9] The Δn_{ij}'s can be calculated according to

$$\Delta n_{ii} = \frac{c_i x_j \bar{V}_j^2}{x_i V}\left(\frac{1-D}{D}\right) \qquad i \neq j$$

$$\Delta n_{12} = -\frac{c_1 \bar{V}_1 \bar{V}_2}{V}\left(\frac{1-D}{D}\right)$$

$$\Delta n_{21} = -\frac{c_2 \bar{V}_1 \bar{V}_2}{V}\left(\frac{1-D}{D}\right) \tag{4}$$

where c_i is the molar concentration of component *i*, $\bar{V}_i$ is the partial molar volume of component *i*, and $D = (x_2/RT)((\partial\mu_2/\partial x_2))_{T,P}$. Figure 5 shows the Δn_{ji}'s for the present system at 298.15 K. This confirms that both the DO and the BDO molecules tend to be surrounded by molecules of the other species because $\Delta n_{ii} < 0$, whereas Δn_{ij} $(i \neq j) > 0$ over the whole composition range. This means that at the interface a molecule of DO will be surrounded by more molecules of DO than what would correspond to a random bulk mixture; in the bulk, there is a depletion of DO molecules around each DO molecule with respect to a random bulk mixture. However, it has to be stressed that the values of Δn_{ij} obtained for this mixture (except those of Δn_{11}) are rather close to the experimental limit of the light-scattering technique, and probably more precise data would be obtained from small-angle X-ray scattering.

Comparison with the Predictions of a Lattice-Fluid Model. Although several molecular models have been proposed to predict the surface tension,[3,4,30,31] and reasonable results have been obtained for pure components,[31,32] the estimation of Γ_{12} for real complex mixtures using rigorous statistical mechanical

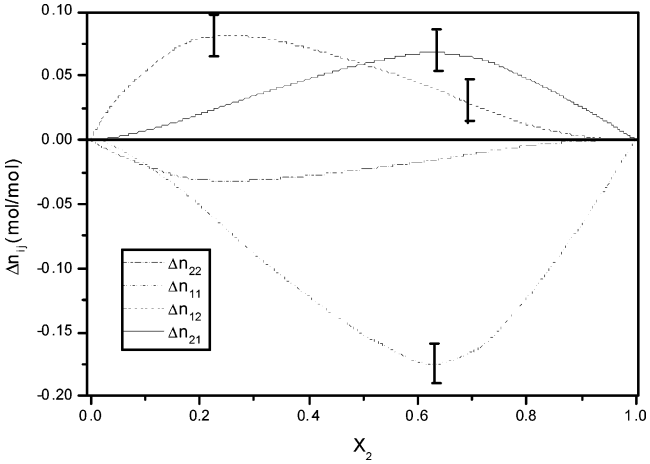

Figure 5. Bulk local concentrations Δn_{ij} calculated according to eq 4. Heterocoordination is indicated by the fact that $\Delta n_{ii} < 0$, whereas Δn_{ij} $(i \neq j) > 0$.

theories is not satisfactory yet. Therefore, in this section, we will focus on the prediction of $(\partial\mu_2/\partial x_2)$. To this end, it is possible to use any theory suitable for the prediction of the bulk thermodynamic properties of the mixtures. This is due to the fact that equilibrium conditions impose the condition that the chemical potential of any component at the interface has to be the same as that in any of the coexisting bulk phases. In this work, we will test the lattice-fluid model developed by Panayiotou and Sanchez for hydrogen-bonded mixtures.[21,33] This theory has been found to give a reasonable description of the bulk properties of nonaqueous mixtures.[34] In the present work, we will give only the equation of state (EoS) and the equations that account for the hydrogen bonds.

The EoS is

$$\tilde{P} + \tilde{\rho}^2 + \tilde{T}\left[\ln(1-\tilde{\rho}) + \tilde{\rho}\left(1 - \frac{1}{\tilde{r}}\right)\right] = 0 \tag{5}$$

where the reduced variables are defined by $\tilde{P} = P/P^*$, $\tilde{T} = T/T^*$, and $\tilde{\rho} = \rho/\rho^*$, with P^*, T^*, and ρ^* being substance-dependent parameters that define the size of the molecules and the van der Waals-type interactions between them. The average number of segments per molecule is defined by

$$\frac{1}{\tilde{r}} = \frac{1}{r} - \nu_H \tag{6}$$

where ν_H is the fraction of hydrogen bonds in the system, and *r* is the average number of segments per molecule.

For pure BDO, we have assumed that the molecules have $d = 2$ donor groups and $a = 2$ acceptor groups, whereas for the DO molecules $d = 1$ and $a = 1$. The model leads to the following equation

$$r\nu_H = \frac{[d + a - \{A_{ij}(A_{ij} + 2(d+a)) + (d-a)^2\}^{1/2} - A_{ij}]}{2} \tag{7}$$

with $A_{ij} = (r/\tilde{\rho})\exp((G_{ij}^0/RT))$ and $G_{ij}^0 = E_{ij}^0 - TS_{ij}^0 + PV_{ij}^0$, where the energy, entropy, and volume are characteristics of the hydrogen bond. We have used for these parameters the same values as in ref 34. The pure-component parameters P^*, T^*, and ρ^* have been obtained from the fit of the P−V−T surface of each pure component to eqs 5−7, and they are given in Table 2.

TABLE 2: Pure-Component Parameters of the Panayiotou−Sanchez Theory for Pure Components[a]

	P^* (MPa)	T^* (K)	ρ^* (kg·mol^{-1})	r
1,4-butanediol	475.2	561.4	1090.4	8.41
1-dodecanol	419.5	536.9	913.6	19.17

[a] Hydrogen-bond parameters: $E^\circ = -25.1$ kJ·mol^{-1}; $S^\circ = -26.5$ J·mol^{-1}·K^{-1}; $V^0 = -5.6 \times 10^{-6}$ m^3·mol^{-1}.

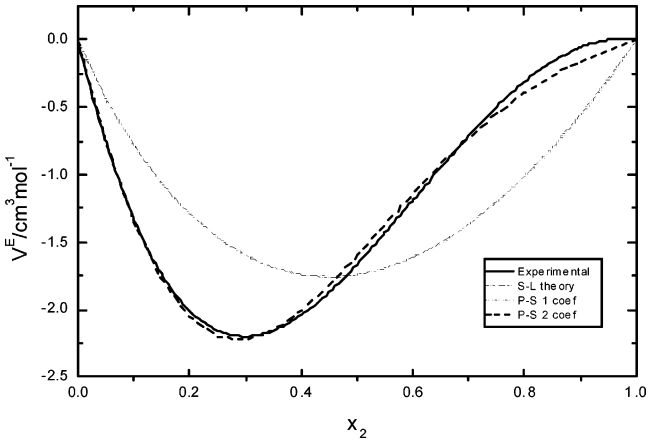

Figure 6. Excess molar volumes V^E obtained from the density measurements, and the predictions obtained with the Panayiotou and Sanchez model: the dashed line us the prediction with one fitting parameter, and the dashed−dotted line is the prediction with two fitting parameters.

For the mixture, it is necessary to account for self- and cross-association, which lead to a system of coupled equations

$$\nu_{ij}A_{ij} = r\left(\frac{N_d^i}{rN} - \sum_{k=i}^{n}\nu_{ik}\right)\left(\frac{N_a^j}{rN}\sum_{k=j}^{m}\nu_{kj}\right) \qquad (8)$$

Two binary parameters, ξ and ζ, have been fit to the P−V−T-x_2 surface of the mixture.[35] ξ takes into account the weakness or strength of the binary interactions with respect to those between like molecules, and ζ takes into account the change in the core volume V^* in the mixture with respect to a linear combination of the pure-component values. Figure 6 shows the best fit of the excess molar volume of the mixture, V^E, for the model. As can be observed, the use of $\zeta \neq 0$ greatly improves the prediction of the volumetric properties.

We have calculated $((\partial\mu_2/\partial x_2))_{T,P}$ using the model of Panayiotou and Sanchez; the ratio of the calculated value to the experimental value obtained from light scattering is equal to the ratio of the calculated value to the experimental value of Γ_{21} because the experimental values of $((\partial\gamma/\partial x_2))_{T,P}$ are used in both cases. This ratio is also an indication of the success of the prediction of the bulk local compositions. Figure 7 shows that the theoretical predictions are not satisfactory despite the fact that the model is able to describe correctly the volumetric properties of the mixture. This behavior arises from the fact that the model predicts an excess Gibbs energy curve that is too skewed toward the low values of x_2, thus leading to values of $((\partial\mu_2/\partial x_2))_{T,P}$ that are larger than the experimental ones for mixtures diluted in DO and lower than the experimental ones for more concentrated mixtures. This stresses the need to be very careful when estimating Γ_{21} from mixture models that are frequently used to calculate the phase equilibrium conditions.

Conclusions

The light-scattering (LS) measurements on the BDO (1)−DO (2) mixture show a clear tendency to heterocoordinate in the bulk. For the BDO molecules, this tendency shows a maximum at $x_2 \approx 0.7$, whereas for the DO molecules, this maximum appears at $x_2 \approx 0.2$. Surprisingly, increasing T increases the overall tendency to teterocoordinate, which may indicate that temperature is more efficient in breaking the hydrogen bonds of the BDO molecules.

Small amounts of DO lead to a drastic decrease in the surface tension, γ, of the mixture in the $0.01 \leq x_2 \leq 0.05$ range and in the temperature interval $293 \leq T\,(\mathrm{K}) \leq 330$. The surface entropy shows a complex concentration dependence that is similar to that found for some water−alcohol mixtures.

Combining the LS and γ results allows one to calculate precise values of the excess adsorption Γ_{21}. The Γ_{21} versus x_2 curve presents a maximum at $x_2 \approx 0.01$ over the whole temperature range studied. The maximum of Γ_{21} is more than 20% lower than the value calculated considering ideal mixture behavior, a difference that increases with T.

We have used the lattice-fluid model of Panayiotou and Sanchez to calculate $(\partial\mu_2/\partial x_2)$. Combining these values with the experimental values of $(\partial\gamma/\partial x_2)$ leads to values of Γ_{21} that differ from the experimental ones by up to 50%, which is surprising because the mixture is only moderately nonideal.

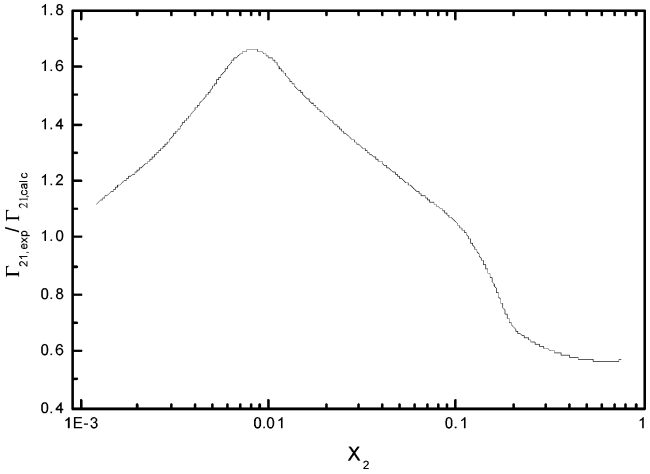

Figure 7. Ratio of the experimental relative adsorption values to those predicted by the Panayiotou and Sanchez model with two fit parameters.

Acknowledgment. This work has been financed in part by MCyT under grants MAT2003-01517, VEM2003-20574-C03-03, and BQU2003-01556 and CAM under grant 07N/0028/2002. We acknowledge the support of the CAI de Espectroscopía (SIRC) of UCM.

Appendix

The osmotic compressibility has been calculated from the light-scattering data according to the following procedure. The Rayleigh ratio, R, has been computed from the intensity of the light scattered by the sample, I, and the intensity of the light scattered by a sample of toluene, I_T. $R = R_T(I/I_T)$, with $R_T = 3.05 \times 10^{-5}$ cm^{-1}.[36] The isotropic contribution to the Rayleigh ratio, R_i is equal to R because, as shown in Figure 1a, I is angle-independent in this system.

According to Walter et al.[37] R_i can be written as

$$R_i = R_d + R_c + R^* \qquad (A.1)$$

where R_c arises from concentration fluctuations, R_d arises from density fluctuations, and R^* is the coupling term between both types of fluctuations. These contributions can be written as

$$R_d = \frac{\pi^2}{2\lambda_0^4} k_B T \kappa_T \left[\rho\left(\frac{\partial \epsilon}{\partial \rho}\right)_T\right]^2$$

$$R_c = \frac{\pi^2}{2\lambda_0^4} k_B T V x_1 \frac{\left(\frac{\partial \epsilon}{\partial x_2}\right)_T^2}{\left(\frac{\partial \mu_2}{\partial x_2}\right)_T} \tag{A.2}$$

$$R^* = \frac{\pi^2}{2\lambda_0^4} k_B T \rho \left(\frac{\partial \epsilon}{\partial \rho}\right)_T x_1 x_2 \left(\frac{\partial \epsilon}{\partial x_2}\right)_T$$

with $\epsilon \approx n^2$ and

$$\rho\left(\frac{\partial \epsilon}{\partial \rho}\right)_T = \frac{2n(n^2-1)(n+0.4)}{n^2+1+0.8n} \tag{A.3}$$

Here λ_0 is the wavelength of incident light in vacuum, κ_T is the isothermal compressibility, ρ is the density, V is the molar volume of the mixture, ϵ is the high-frequency permittivity, and n is the refractive index.

S_{cc} can be calculated from the experimental data through

$$S_{cc} = x_1 x_2 \frac{R_c}{R_{id}} \tag{A.4}$$

with $R_{id} = (\pi^2/2\lambda_0^4)\, k_B T V x_1 x_2 (\partial \epsilon / \partial x_2)_T^2$; S_{cc} is related to $(\partial \mu_2 / \partial x_2)_T$ through eq 2.

References and Notes

(1) Adamson, A. W.; Gast, A. P. *Physical Chemistry of Surfaces*, 6th ed.; Academic Press: New York, 1999.

(2) Papaioannou, D.; Magopoulou, A.; Talilidou, M.; Panayiotou, C. *J. Colloid Interface Sci.* **1993**, *156*, 52.

(3) Teixeira, I. C.; Almeida, B. S.; Telo da Gama, M.; Rueda, J. A.; Rubio, R. G. *J. Phys. Chem.* **1992**, *96*, 8488.

(4) Gloor, G. J.; Blas, F. J.; Martín del Río, E.; De Miguel, E.; Jackson, G. *Fluid Phase Equilib.* **2002**, *194−197*, 521.

(5) Bathia, A. B.; Thornton, D. E. *Phys. Rev. B* **1970**, *2*, 3004.

(6) Rubio, R. G.; Prolongo, M. G.; Díaz Peña, M.; Renuncio, R. A. R. *J. Phys. Chem.* **1987**, *91*, 1177.

(7) Davis, H. T.; *Statistical Mechanics of Phases, Interfaces, and Thin Films*; VCH: New York, 1996.

(8) Andreoli-Ball, L.; Costas, M.; Patterson, D.; Rubio, R. G.; Masegosa, R. M.; Cáceres, M. *Ber. Bunsen-Ges. Phys. Chem.* **1989**, *93*, 882.

(9) Ruckenstein, E.; Shulgin, I. *J. Phys. Chem. B* **1999**, *103*, 872.

(10) Shulgin, I.; Ruckenstein, E. *J. Phys. Chem. B* **1999**, *103*, 10266.

(11) Strey, R.; Viisanen, Y.; Aratono, M.; Kratohvil, J. P.; Yiu, Q.; Friberg, S. E. *J. Phys. Chem. B* **1999**, *103*, 9112.

(12) Prausnitz, J. M.; Lichtenthaler, R. N.; Gomes de Azevedo, E. *Molecular Thermodynamics of Fluid Phase Equilibria*, 3rd ed.; Prentice-Hall: Englewood Cliffs, NJ, 1999.

(13) Almásy, L.; Cser, L.; Jancsó, G. *J. Mol. Liq.* **2002**, *101*, 89.

(14) Glinski, J.; Chavepeyer, G.; Platten, J.-K. *J. Chem. Phys.* **1999**, *111*, 3233; Glinski, J.; Chavepeyer, G.; Platten, J.-K. *Chem. Phys.* **1999**, *272*, 119.

(15) Lavi, P.; Marmur, A. *J. Colloid Interface Sci.* **2000**, *230*, 107.

(16) Gmehling, J.; Onken, U.; Weidlich, U. *Vapor-Liquid Equilibrium Data Collection*; Dechema: Frankfurt, Germany, 1982; Vol. 1.

(17) Gracia-Fadrique, J.; Brocos, P.; Piñeiro, A.; Amigo, A. *Langmuir* **2002**, *18*, 3604.

(18) Brown, W., Ed. *Light Scattering: Principles and Development*; Clarendon Press: Oxford, U.K., 1996.

(19) Zielkiewicz, J. *Phys. Chem. Chem. Phys.* **2003**, *5*, 1619.

(20) Narayanan, T.; Pitzer, K. S. *Phys. Rev. Lett.* **1994**, *73*, 3002.

(21) Panayiotou, C.; Sanchez, I. C. *J. Phys. Chem.* **1991**, *95*, 10090.

(22) Hugglin, M. B., Ed. *Light Scattering from Polymer Solutions*; Academic Press: London, 1972.

(23) Muñoz, M. G.; Monroy, F.; Ortega, F.; Rubio, R. G.; Langevin, D. *Langmuir* **2000**, *16*, 1083.

(24) Riddick, J. A.; Bunger, W. B. *Organic Solvents: Physical Properties and Methods of Purification*, 3rd ed.; Techniques of Chemistry, Vol. II; Wiley-Interscience: New York, 1970.

(25) Matteoli, E. *J. Phys. Chem. B* **1997**, *101*, 9800.

(26) Lyklema, J. *Fundamentals of Interface and Colloid Science*; Academic Press: San Diego, CA, 1995; Vol. II.

(27) Glinski, J.; Chavepeyer, G.; Platten, J.-K. *J. Chem. Phys.* **1999**, *111*, 3233. Glinski, J.; Chavepeyer, G.; Platten, J.-K. *J. Chem. Phys.* **1998**, *109*, 5050.

(28) Glinski, J.; Chavepeyer, G.; Platten, J.-K. *Chem. Phys.* **2001**, *272*, 119.

(29) Jerie, K.; Baranowski, A.; Glinski, J.; Przybylski, J. *J. Radioanal. Nucl. Chem.* **2003**, *257*, 367.

(30) Winkelmann, J. *J. Phys.: Condens. Matter* **2001**, *13*, 4739.

(31) Enders, S.; Quitzsch, K. *Langmuir* **1998**, *14*, 4606.

(32) Escobedo, J.; Mansoori, G. A. *.AIChE J.* **1996**, *42*, 1425.

(33) Luengo, G.; Rubio, R. G.; Sanchez, I. C.; Panayiotou, C. *Macromol. Chem. Phys.* **1994**, *195*, 1043.

(34) Colín, A. C.; Rubio, R. G.; Compostizo, A. *Polymer* **2000**, *41*, 7407.

(35) Compostizo, A.; unpublished work, 2003.

(36) Bender, T. M.; Lewis, R. J.; Pecora, R. *Macromolecules* **1986**, *19*, 244.

(37) Walter, A.; van Dijk, F.; van Dijk, M. A. *Macromolecules* **1993**, *26*, 5088.